Journal of the Taiwan Institute of Chemical Engineers 173 (2025) 106161

Contents lists available at ScienceDirect

Journal of the Taiwan Institute of Chemical Engineers

journal homepage: www.journals.elsevier.com/journal-of-the-taiwan-institute-of-chemical-engineers

Eco-friendly green inhibitor for corrosion protection of API 5L X60 carbon steel in sulfuric acid solution

Sobhi Nour El Houda [a,b,*], Boukhouiete Amel [c]

[a] Departement of chemistry, Water and Environment Science and Technology Laboratory, Mohamed, Cherif Messaadia University, Souk-Ahras, Algeria
[b] Laboratory of energy and electrochemistry of solid (LEES), University Ferhat Abbas Setif 1, Setif, Algeria
[c] Departement of chemistry, university Badji-Mokhtar, Annaba, Algeria

ARTICLE INFO

Keywords:
API5LX60 steel
Sulphuric acid
Olibanum
Inhibitor
Corrosion

ABSTRACT

Background: Corrosion is a widespread issue affecting metals and alloys across various industries. The use of corrosion inhibitors remains one of the most effective protection methods. Due to growing environmental and health concerns, the focus has shifted toward eco-friendly alternatives.Olibanum has emerged as a promising green corrosion inhibitor with potential applications in industrial environments.

Methods: Temperature effect, Inhibition efficiency, corrosion behaviour and corrosion mechanism of the inhibitors on carbon steel are evaluated using gravimetry and electrochemical techniques (potentiodynamic polarization curves (PDP), electrochemical impedance spectroscopy (EIS), and open circuit potential). Scanning electron microscopy (SEM) and energy dispersive X-ray spectroscopy (EDS) examined the surface morphology. Furthermore, Infrared Spectroscopy (IR) is employed to characterize the inhibitor.

Significant findings: The results show that this natural substance is a mixed-type inhibitor with anodic behavior dominating, with a maximum efficiency of 85% obtained at a concentration of 4 g/L. The inhibition efficiency of Olibanum increased with inhibitor concentration and temperature. The dynamic behavior of Olibanum shows that its adsorption isotherm on steel follows the Temkin type with both physicochemical adsorption processes. The low Ea, moderate ΔHact, and ΔS act values provide that the adsorption appears to be predominantly physical, but there may also be some chemical adsorption. SEM micrographs confirm the presence of a protective layer on the steel surface.

1. Introduction

Corrosion is a silent enemy, a spontaneous and costly degradation process, similar to natural disasters such as earthquakes, floods, and volcanic eruptions, with one crucial difference: while natural disasters are beyond our control, corrosion can be prevented or at least managed [1]. Several effective techniques exist for controlling corrosion, with corrosion inhibitors being the most widely used method for protecting metals and alloys [2]. Corrosion inhibitors play a critical role in minimising or preventing corrosion when added at low concentrations to a corrosive environment. They work by forming a protective film on the metal surface, effectively blocking direct contact between the metal and corrosive agents. These inhibitors are classified based on their origin as either organic or inorganic and their method of production as either synthetic or naturally occurring. Synthetic organic corrosion inhibitors and traditional inorganic corrosion inhibitors such as chromates and lead are known to be subject to restrictive environmental regulations. As a result, researchers are increasingly looking for green alternatives with high corrosion inhibition efficiency and lower costs [3–7]. Examples of these inhibitors include Trifolium repens, Pisum Sativum L. leaves, jasmine flower extract, wood hibiscus leaf extract, Capsicum annuum L. leaf extract, Vang tea water extract, Fatsia japonica leaf extract, Barringtonia acutangula flower water extract, Chinese mahonia leaves, Glebionis coronaria L. flower extract, Dillenia suffruticosa leaves, Arum dioscoridis plant leaf extract, Gum Arabic, Justicia brandegeeana [8–21] and many others. These inhibitors offer numerous benefits, including environmental sustainability and human health safety. Derived from natural sources, they are biodegradable and pose minimal environmental risks compared to traditional synthetic inhibitors. In addition, they are highly effective in preventing metal corrosion, making them a

* Corresponding author at: Laboratory of water and Environment Science and Technology, Mohamed Cherif Messaadia University, Souk-Ahras, Algeria, Laboratory of energy and electrochemistry of solid (LEES), University Ferhat Abbas 1, Setif, Algeria.
E-mail address: n.sobhi@univ-soukahras.dz (S.N.E. Houda).

https://doi.org/10.1016/j.jtice.2025.106161
Received 11 February 2025; Received in revised form 20 April 2025; Accepted 21 April 2025

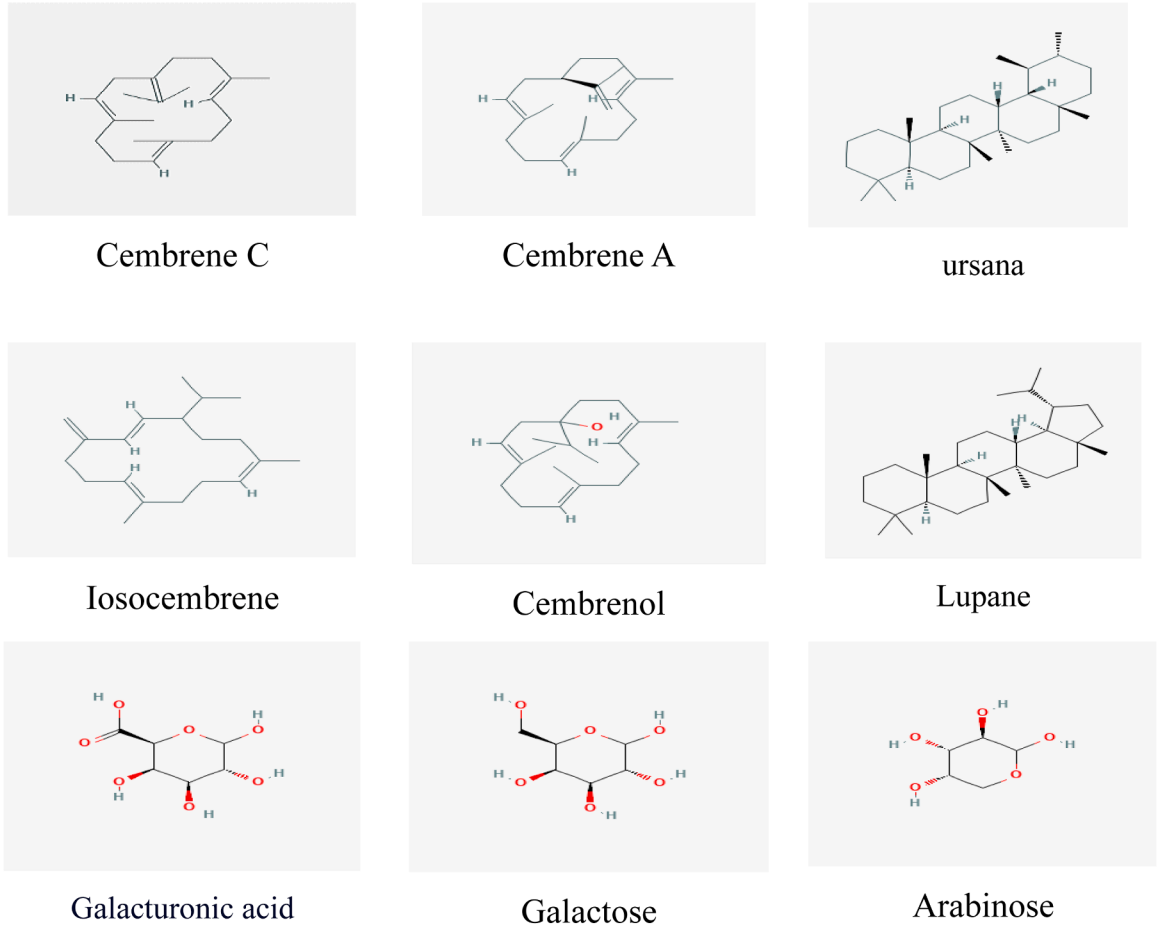

Fig. 1. Example of some structures isolated from Olibanum [28].

promising solution for industrial applications seeking environmentally friendly corrosion protection strategies.

In this study, Olibanum, a natural resin known for its rich composition of bioactive compounds, was investigated as a green corrosion inhibitor for API 5L X60 carbon steel in 0.5M sulphuric acid solution. Compared to other green inhibitors, Olibanum contains a unique blend of terpenoids, resin acids and essential oils, which contribute to its strong adsorption on the metal surface and enhance its inhibition performance. Corrosion performance was evaluated using Tafel polarisation curves, electrochemical impedance spectroscopy (EIS) and open circuit potential (OCP) measurements. In addition, surface morphology was characterised using scanning electron microscopy (SEM) and energy dispersive X-ray spectroscopy (EDS). The infrared spectroscopy (IR) characterize the functional group in Olibanum. The effect of temperature was also investigated to assess its influence on the adsorption behaviour and inhibition efficiency, providing deeper insights into the stability and effectiveness of Olibanum as a sustainable corrosion inhibitor.

Olibanum, also called Frankinsence, is an aromatic resin obtained from trees of the genus Boswellia. Boswellia is a genus of trees known for their fragrant resin. Olibanum is an extract from the resin of the tree. There are four main following species of Boswellia which produce true Olibanum and resin is available in various grades. The grades depend on the time of harvesting. Moreover, it is in hand sorted for quality.

As shown in Fig. 1, it is composed of Olibanum gum, resin acids, and volatile oils, with key chemical components including Boswellia acid, 3-acetyl-bêta-boswellic acid, alpha-boswellic acid, 4-O-methyl-glucuronic acid, and incensole acetate. Historically, Olibanum has been widely used in various traditional medical systems, especially in Ayurveda, where it has been employed to aid digestion, promote skin health, and treat arthritis. It is particularly valued for its anti-inflammatory properties, making it effective in managing conditions like rheumatoid arthritis, asthma, and other inflammatory disorders.

Beyond its medicinal benefits, Olibanum is highly regarded in perfumery, aromatherapy, and religious ceremonies for its pleasant aromatic smoke. The extraction process involves using ether to isolate the resin, followed by drying and size reduction. Additionally, Olibanum has significant pharmacological applications, serving as an anti-inflammatory agent for gastrointestinal treatments and as a material for developing microcapsules for controlled drug delivery [22–27].

This study is the first to investigate the use of Olibanum as a green corrosion inhibitor for API5LX60 carbon steel in 0.5M sulfuric acid. It investigates the ability of the plant to provide protection under acidic conditions, with the aim of demonstrating its effectiveness as a sustainable alternative to traditional inhibitors and promoting the widespread adoption of green corrosion protection strategies for industrial applications.

2. Experimental details

Electrochemical measurements were performed using a PGZ301 potentiostat (controlled by VoltaMaster 40 software) in a standard three-electrode configuration, employing potentiodynamic polarization and electrochemical impedance spectroscopy (EIS). The working electrode (WE) was the API 5L X60 sample. Its chemical composition (in weight percent) includes maximum 0.102% carbon, 1.06% manganese, 0.34% minimum silicon, 0.018% maximum phosphorus, 0.17% maximum sulfur, 0.18% maximum nickel, 0.019% maximum niobium,

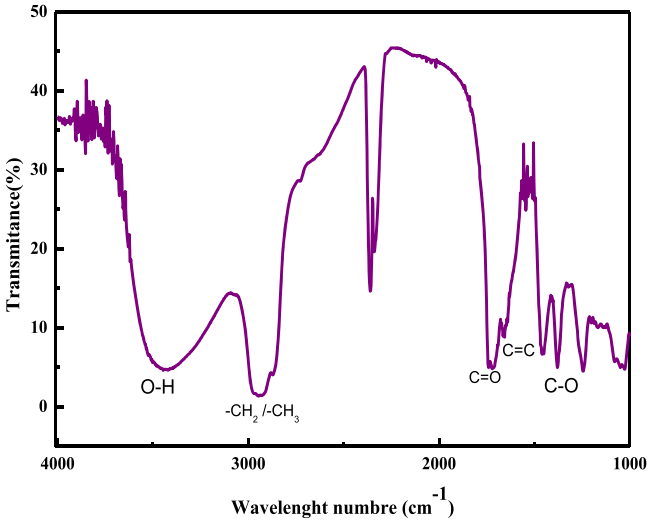

Fig. 2. The IR analyses of Olibanum.

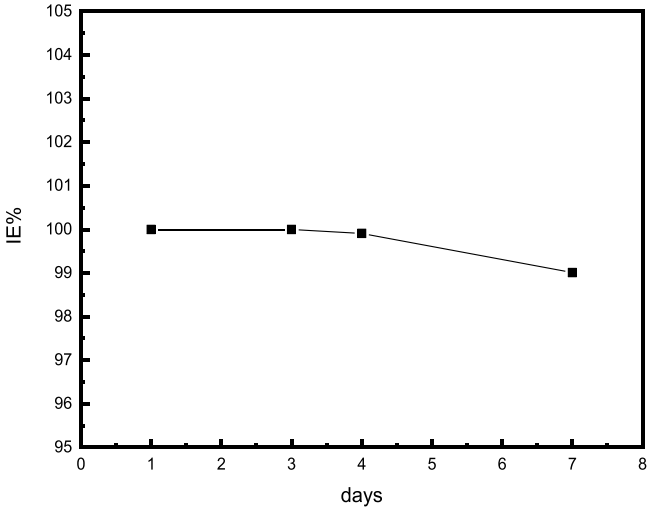

Fig. 3. Variation of Inhibition Efficiency (IE%) with immersion Time.

Table 1
Characteristics of the relationship between immersion time and IE%.

Time(h)	Δm (g)	Vcorr (g.cm^{-2}.h)	IE (%)
24	**0**	**0**	100
72	**0**	**0**	100
120	**1.317×10^{-5}**	**4.457×10^{-17}**	99.91
168	1.469×10^{-4}	2.849×10^{-16}	99.01

and 0.023% maximum titanium, with the rest being iron, while the counter electrode (CE) was platinum and the reference electrode was Ag/AgCl. Following the impedance study, polarisation measurements were carried out on the same test coupon without any further surface preparation.

EIS was carried out in the frequency range 100 kHz to 10 mHz using a 10 mV AC signal. The open circuit potential (OCP) was monitored for 30 min to ensure stability. Potentiodynamic polarisation measurements were performed by scanning the electrode potential from -700 mV to -300 mV relative to the Ag/AgCl reference at a scan rate of 0.5 mV/s, this slow scan rate allowed for testing in quasi-stationary conditions. The tests were conducted in the acidic solution both with and without various concentrations of the Olibanum inhibitor (1-5 g/L), where the

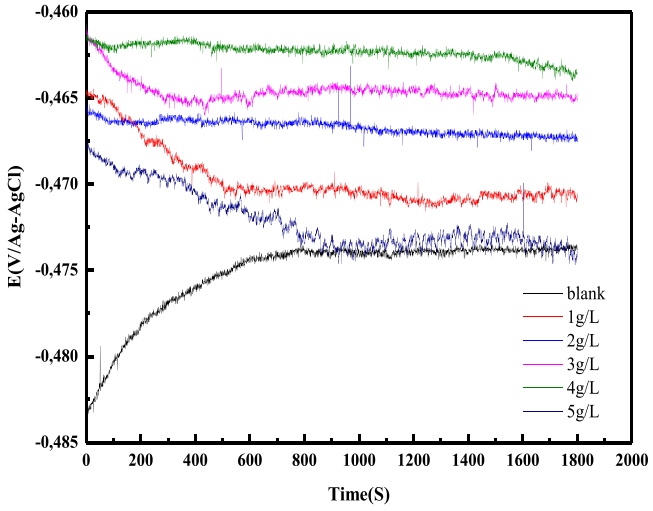

Fig. 4. Open circuit potential (OCP) curves for API5L X60 steel in 0.5 H_2SO_4 solutions with different concentration of inhibitor at 25°C.

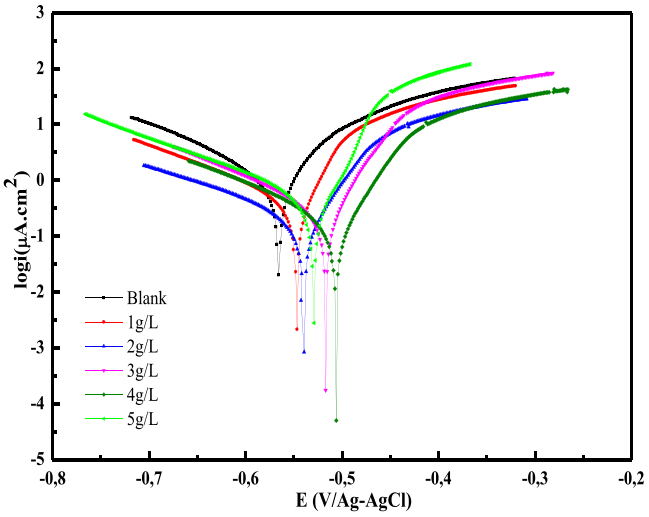

Fig. 5. Potentiodynamic polarization curves for API5LX60 steel in 0.5 M H_2SO_4 in the absence and presence of various concentrations of the inhibitor.

Table 2
Electrochemical parameters for API5LX60 steel in 0.5 M H_2SO_4 solutions in the absence and presence of Olibanum obtained from PDP experiments.

C (g/L)	E_{corr} (mV)	I_{corr} (mA /cm^2)	RP (Ω. cm^2)	βa (mV/dec)	-β c (mV/dec)	IE%
0	**-570**	**0.7139**	**16.5**	**77.9**	**151.0**	/
1	**-530**	**0.3081**	**38.5**	**56.3**	**147.8**	56.84
2	**-516**	**0.2593**	**51.2**	**62.4**	**167.6**	63.68
3	**-493**	**0.1567**	**81.7**	**57.6**	**142.9**	78.05
4	**-468**	**0.1045**	**107**	**52.4**	**135.3**	85.36
5	-501	0.2082	53.2	56.4	129.3	70.84

inhibitor solutions were prepared directly by dissolving its powdered form in the 0.5 M sulfuric acid solution. The inhibition efficiency (IE %) was calculated from polarization data using the corrosion current density (*icorr*) with the following equation:

$$IE_{\%} = \frac{Icorr \; - -Icorr(inh)}{Icorr} \times 100 \qquad (1)$$

Where *Icorr (inh)* and *Icorr* are the inhibited and the uninhibited

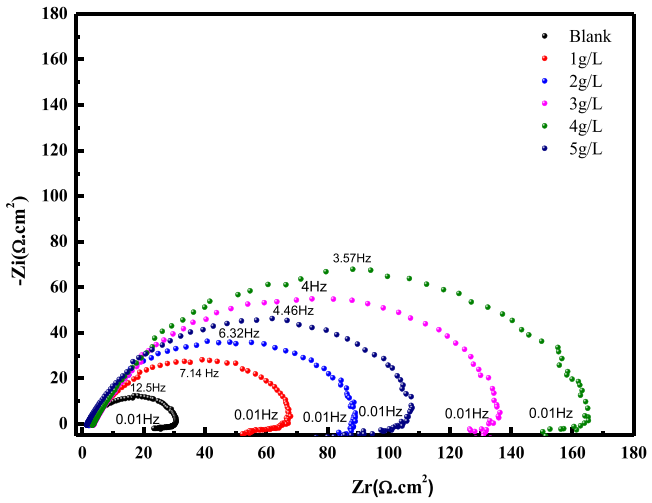

Fig. 6. Nyquist plots for API5LX60 steel in 0.5 M H_2SO_4 solutions in the absence and presence of Olibanum.

corrosion current densities, respectively.

Inhibition efficiency IE % is calculated from impedance data on the basis of the equation:

$$IE_{\%} = \frac{Rtc - Rs}{Rtc} \times 100 \quad (2)$$

Where *Rtc* and *Rs* are the charge transfer resistance values in the presence and the absence of the inhibitor, respectively.

The Gravimetric method consists of measuring the mass loss (Δw) of a surface sample (S) during a period (t) of immersion in a corrosive solution at a constant temperature [2].

The corrosion rates calculated using the following formula:

$$V_{corr} = \frac{\Delta w}{S.t} \quad (3)$$

ΔW : is the weight loss (g), S : is the specimen surface area in (cm^2), and t represent the immersion time (h). Vcorr is the corrosion rate expressed in ($g.cm^{-2}.h$).

To determine the inhibition efficiency (IE%), we used Equation (4) :

$$IE\% = \frac{V_{corr} - V_{inh}}{V_{corr}} \times 100 \quad (4)$$

IR spectra were acquired using a PerkinElmer Spectrum Series FTIR Fourier Transform instrument. The sample was prepared as a KBr pellet, in which the product was dispersed at a 3% concentration in 150 mg of pre-dried KBr and pressed under 80 tons/cm^2 to characterize the functional groups present in Olibanum. The analysis was conducted to identify and analyze the molecular vibrations associated with specific functional groups, providing insights into the chemical composition and structural properties of the sample. The instrument was calibrated prior to measurements to ensure accuracy, and the spectra were recorded in the range of 4000 to 400 cm^{-1}. This high-resolution analysis enabled the detailed identification of key functional groups.

The surface morphology was examined using a Thermo Fisher Scientific Quattro scanning electron microscope (SEM) equipped with an

Fig. 8. Electric circuit used to simulate EIS data.

Table 3
Impedance data forAPI5L X60 steel in 0.5 M H_2SO_4 solutions in the absence and presence of Olibanum.

C(g/L)	Rs(Ω. cm^2)	RP (Ω. cm^2)	CPE_{dl}(mF. Cm^2) $\times 10^{-3}$	n	χ^2	IE(%)
0	**3.779**	**27.22**	**0.580**	**0.887**	**0.061**	/
1	**3.599**	**64.17**	**0.489**	**0.903**	**0.055**	57.58
2	**3.562**	**85.17**	**0.484**	**0.907**	**0.212**	68.04
3	**2.967**	**140.5**	**0.463**	**0.803**	**0.320**	80.63
4	**2.353**	**170.8**	**0.432**	**0.796**	**0.222**	84.06
5	2.380	107	0.452	0.891	0.281	74.56

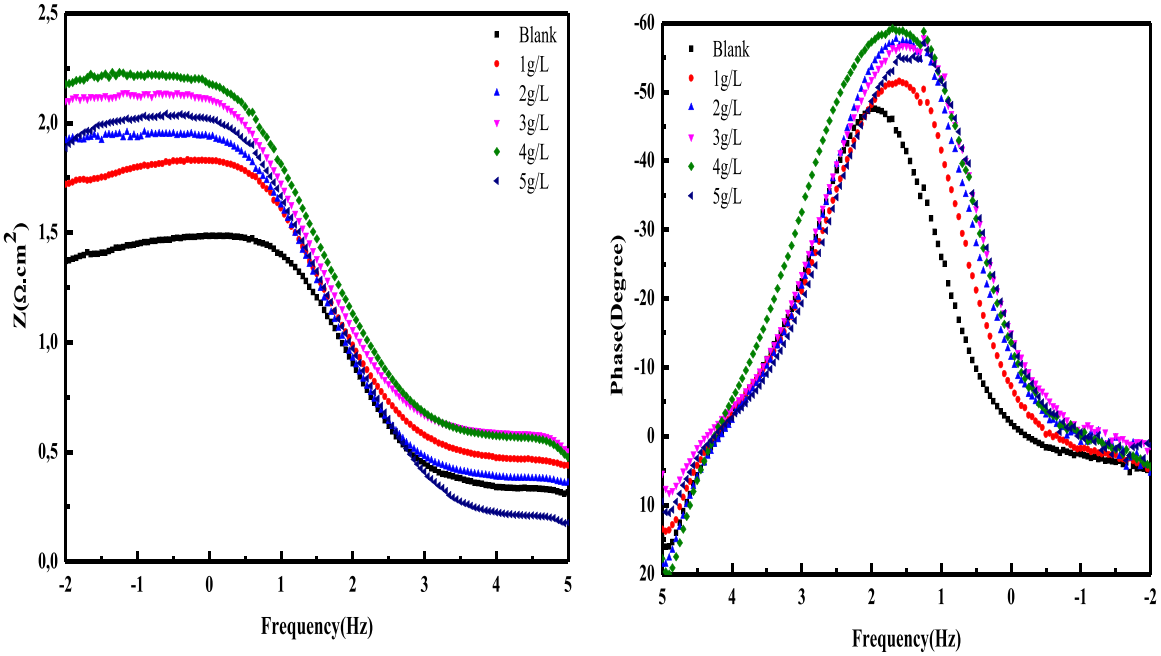

Fig. 7. EIS plots for API5LX60 in 0.5M H_2SO_4 solution without and with different concentrations of Olibanum in Bode modulus.

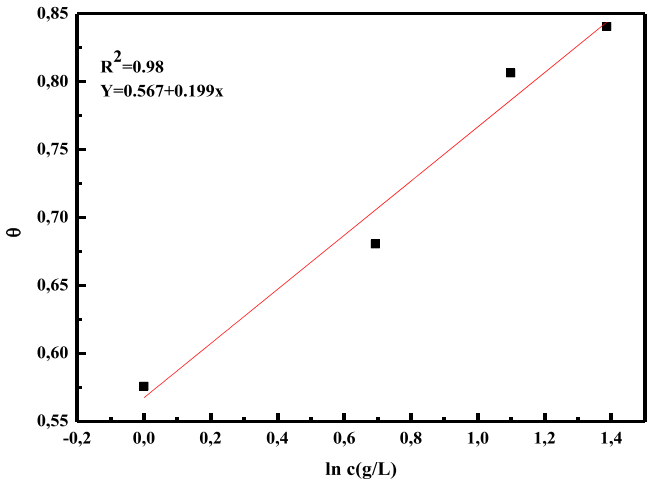

Fig. 9. Temkin isotherm for the degree of surface coverage versus concentration of inhibitor in 0.5M H_2SO_4.

EDAX energy-dispersive X-ray spectroscopy (EDS) system, enabling high-resolution imaging and elemental analysis of the sample.

3. Result and discussions

3.1. Inhibitor characterization

a. Characterization of Olibanum by infrared spectroscopy IR

IR spectroscopy can quickly identify various functional groups, such as hydroxyl, Amino, and carbonyl. This technique is also valuable for analyzing reactions involving the transformation of functional groups in polymers [29]. Fig. 2 displays the infrared (IR) spectrum of Olibanum.

The IR spectrum analysis of Olibanum reveals the presence of several functional groups, indicating its complex chemical composition. The broad absorption band observed between 3400-3200 cm^{-1} corresponds to O-H stretching, likely due to hydrogen bonding. The peak around 2925 cm^{-1} is associated with aliphatic C-H stretching, while the absorption near 1740 cm^{-1} indicates C=O stretching, characteristic of carboxylic acids or esters. A peak around 1600 cm^{-1} suggests C=C stretching, typical of alkenes. Further, C-H bending vibrations are evident around 1450 cm^{-1} for methylene groups and approximately 1375 cm^{-1} for methyl groups. The presence of C-O stretching is identified near 1220 cm^{-1}, corresponding to ether or alcohol functional groups, while the range of 1160-1020 cm^{-1} also reflects C-O stretching, specifically related to esters.

3.2. Gravimetric measurements

Fig. 3 and Table 1 show the results obtained by the gravimetric method in 0.5 M H_2SO_4, with and without the addition of Olibanum at a concentration of 4 g/L.

The inhibition efficiency values show a stability that is accompanied by an increase in immersion time. This stability indicates that the formation of the protective film remains constant over time.

3.3. Electrochemicals studies

3.3.1. Open circuit potential (OCP)

Samples of API 5L X60 steel were immersed in a sulphuric acid solution for 30 minutes. These experiments were carried out with and without the inclusion of Olibanum. Observations were made of the variations in open circuit potential (OCP) values compared to uninhibited solutions at different inhibitor concentrations. The results obtained are described in Fig. 4.

Examination of the OCP curves in Fig. 4 shows that the potential is stable from the first few seconds. It is clear that the potential shifts towards more positive values compared to the uninhibited medium, confirming the formation of a protective film [30]. It was also observed that the potential remained stable for the duration of the immersion at 4 g/L, indicating that the protection at this concentration was very high. The stability of the potential in the sulfuric acid medium is related to the formation of oxide or hydroxide layers on the surface, which provide temporary stability of the potential.

3.3.2. Potentiodynamic polarization

Fig. 5 depicts potentiodynamic polarization curves for API5LX60 steel immersed in 0.5 M H_2SO_4 at room temperature, both with and without the addition of different concentrations of Olibanum.

Polarization curves were generated to visualise the effect of the adsorbed components of Olibanum on the anodic and cathodic branches of the polarisation curve. The main polarisation parameters obtained using the Tafel extrapolation method, including corrosion current density (icorr), corrosion potential (Ecorr), cathodic Tafel slope (βc) and anodic Tafel slope (βa) are summarized in Table 2. In addition, the inhibition efficiency (IE%) at different Olibanum concentrations, derived from the icorr values, is shown in Table 2.

The results show that increasing the concentration of Olibanum from 1 g/L to 4 g/L progressively reduces icorr, indicating suppression of X60 steel dissolution in the presence of the inhibitor. A simultaneous increase in IE% reveals an inverse relationship between icorr and IE% [31]. However, the variations in βa and βc suggest that the addition of Olibanum affects the kinetics of both anodic and cathodic reactions, indicating that Olibanum acts as a mixed-type inhibitor. Furthermore, a positive (more anodic) shift in Ecorr was observed at different Olibanum concentrations, and the shifts in Ecorr values are less than 85 mV compared to the sulphuric acid solution, indicating mixed-type inhibition with a more predominant effect on the anodic behavior [32–34].

3.3.3. Electrochemical impedance spectroscopy (EIS)

To complete the comprehension of the corrosion and inhibition mechanisms of steel API5LX60 in 0.5 M H_2SO_4 in the absence and presence of Olibanum inhibitor, electrochemical impedance measurements were performed.

The results obtained from Nyquist plots, Bode plots, and the equivalent circuit model used to fit the impedance data for carbon steel in 0.5 M H_2SO_4, both without and with different concentrations of Olibanum, are shown in Figs. 6-8. Table 3 summarizes the key parameters, including the inhibition efficiency (IE%) derived from the polarization resistance (Rp) values.

The Nyquist plots show individual capacitive loops that deviate from perfect semicircles and appear slightly depressed below the real axis. This is attributed to frequency dispersion and surface irregularities or heterogeneities. As the Olibanum concentration increases, the diameter of these loops increases, indicating greater inhibition of the charge transfer process at the steel surface.

The corrosion behavior of carbon steel can be modeled using an equivalent circuit consisting of Rp (charge transfer resistance) and Cdl (double layer capacitance) in parallel with Rs (solution resistance). For a more accurate fit, a constant phase element (ZCPE) replaces the traditional Cdl to account for deviations from ideal capacitive behavior.

$$Z_{CPE} = \frac{1}{Y_0(j\omega)^n} \quad (5)$$

Where, Y_0 = proportional factor, j = imaginary unit (value is equal to $\sqrt{-1}$), ω = angular frequency in rad s-1 (ω = 2Π *f* max) and n = phase shift and tells the extent of deviation from ideal behavior. For n = 0, ZCPE represents a resistance with R = Y_0 -1, for n = 1 a capacitance with C-Y_0 and for n = -1 an inductance with L = Y0-1. The Cdl can be calculated by the following equation:

$$C_{dl} = Y_0(\omega_{max})^{n-1} \quad (6)$$

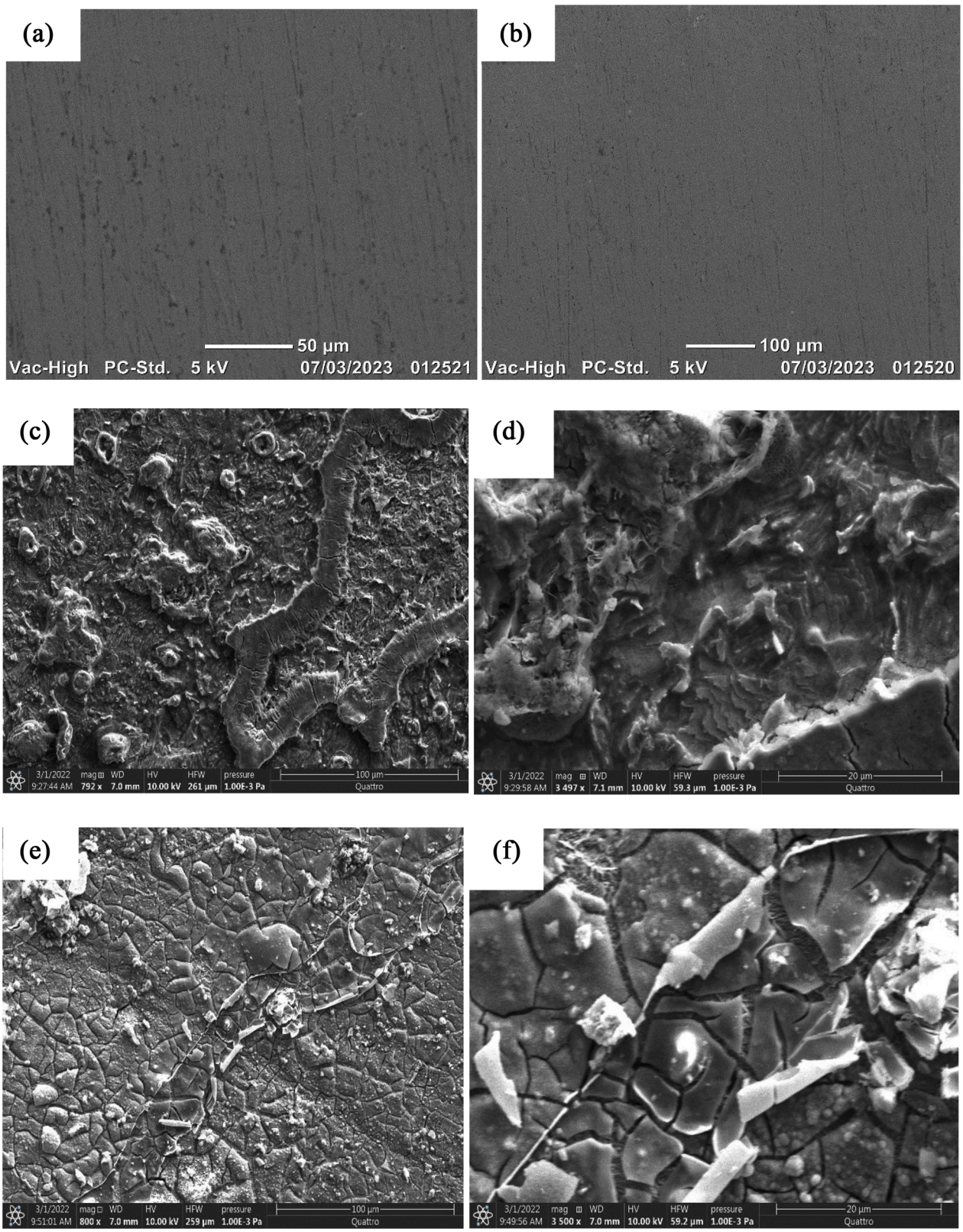

Fig. 10. SEM micrographs of API5LX60 steel electrodes after 3 days, (a, b) steel without immersion;(c, d) in 0.5M H_2SO_4;(e, f) in 0.5M H_2SO_4 solution with inhibitor at 4g/L.

Where ωmax = 2π*f*max (*f*max = maximum frequency of imaginary component of impedance) [33]. The values of Rp and Cdl are influenced by the density of the monolayer formed by the inhibitor molecules. A larger semicircle diameter is observed when the monolayer is densely packed, resulting in an increase in Rp and a decrease in Cdl, thus providing improved corrosion protection.In addition, Rp increases at higher Olibanum concentrations due to improved surface coverage by inhibitor molecules. At the same time, Cdl decreases as water molecules

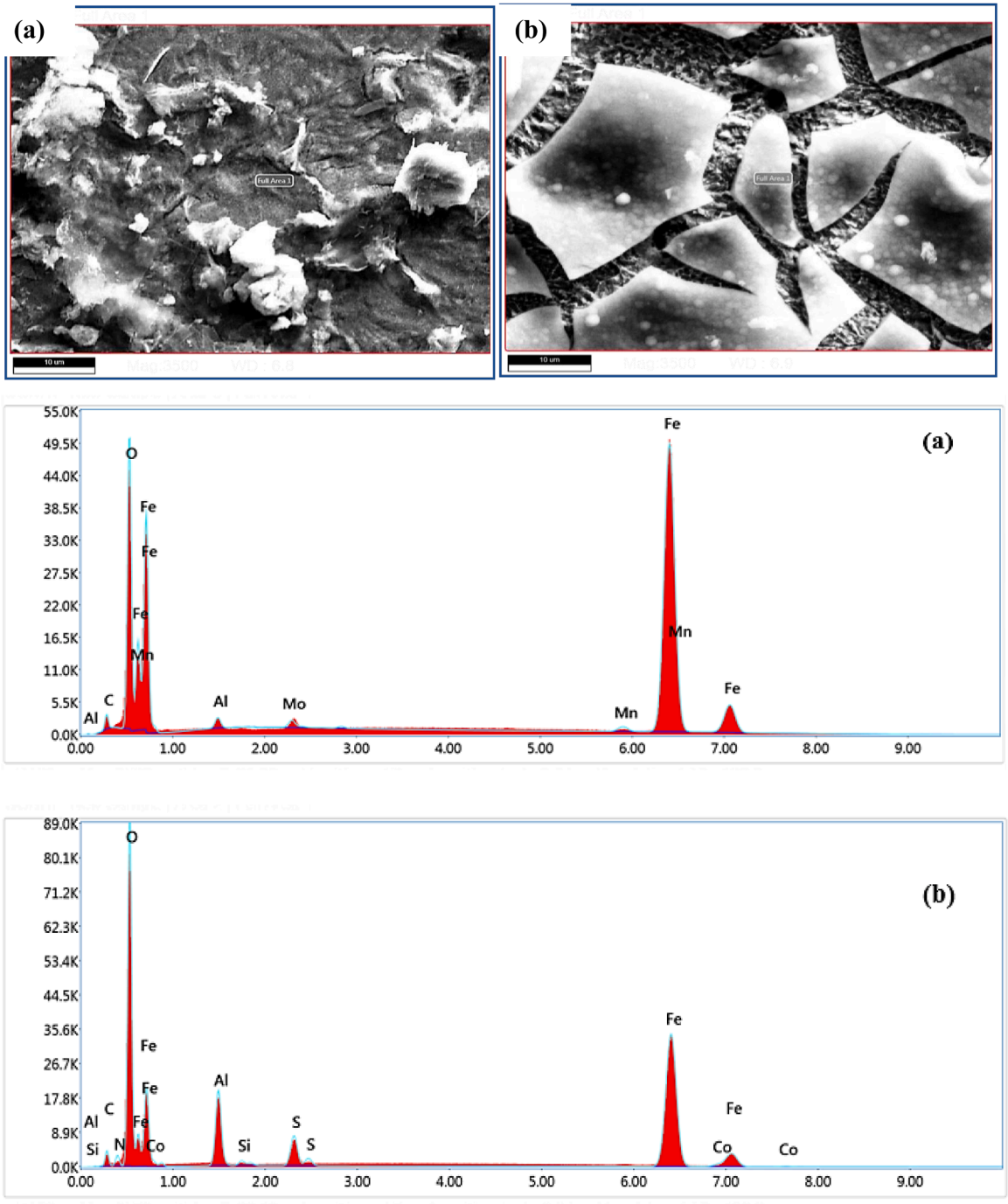

Fig. 11. The SEM- EDX spectra after 72h immersion (a) blank (b) with inhibitor 4g/L.

Table 4
Content of elements obtained from EDS spectra for API 5L X60 carbon steel.

Element	Inhibitor (W %)	Blank (W %)
C	**18.78**	8.34
O	**43.64**	26.91
Fe	34.33	62.42

at the X60/electrolyte interface are replaced by inhibitor molecules, resulting in a lower local dielectric constant and a thicker electrical double layer [35,36].The χ^2 value, which reflects the quality of the equivalent circuit fit, confirms that the proposed circuit is well fitted [37]. Bode plots indicate that the corrosion process proceeds through a single step corresponding to a single time constant. This implies that although the inhibitor does not exhibit ideal capacitive behaviour, it tends towards ideality despite surface deviations along its path [38].

3.4. Adsorption isotherm

Fig. 9 illustrates the Temkin isotherm, which shows the relationship between the degree of surface covering and the concentration of the inhibitor in a 0.5 M H_2SO_4 solution. The Temkin isotherm is employed to examine the adsorption behavior of an inhibitor molecule on the surface of API5LX60 steel. The following equation (7) gives it:

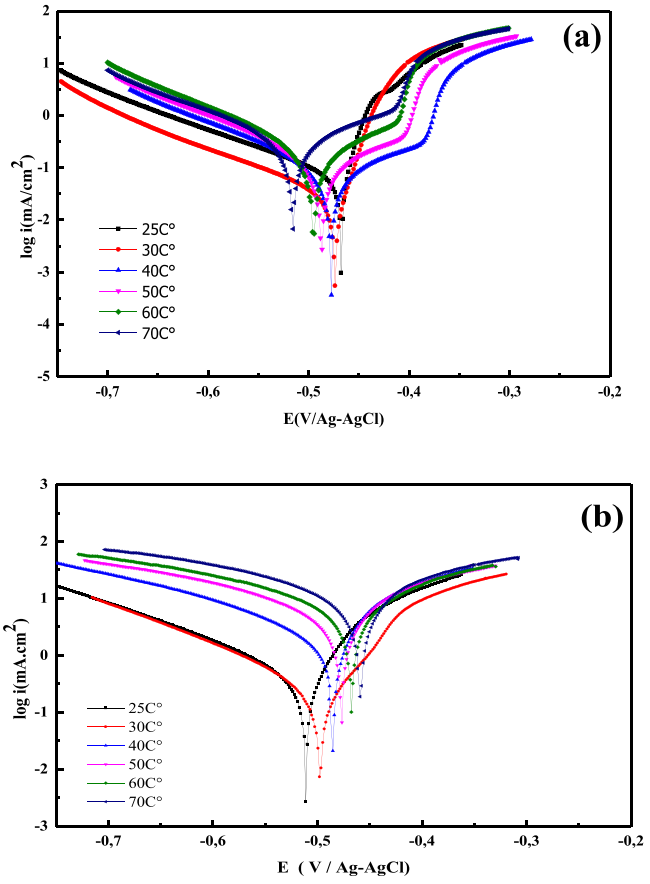

Fig. 12. Polarization curves of API5L X60 carbon steel;(a) API5L X60 carbon steel in 0.5 M H_2SO_4 + 4 g/L inhibitor at different temperatures;(b) in 0.5 M H_2SO_4 without inhibitor at different temperatures.

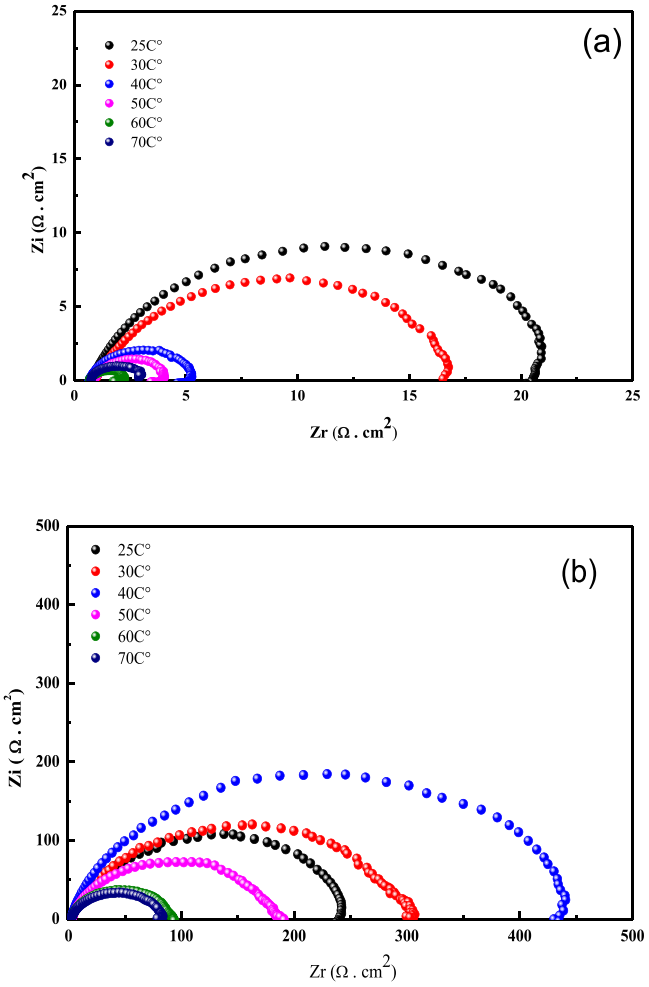

Fig. 13. Nyquist diagrams of API5L X60 carbon steel;(a) in 0.5 M H_2SO_4 without inhibitor at different temperatures;(b) Nyquist diagram of API5L X60 carbon steel in 0.5 M H_2SO_4 + 4 g/L inhibitor at different temperatures.

Table 5
Effect of temperature on the electrochemical parameters of API5LX60 carbon steel in 0.5 M H_2SO_4 in the absence of inhibitor.

Medium/conc		E_{corr}(V)	I_{orr}(mA /cm^2)	R_P (ohm. cm^2)	β_a (m V)	-β_c (m V)
H_2SO_4	25C°	-0.570	0.713	16.5	77.6	151.0
	30C°	-0.498	1.811	12.6	67.8	134.9
	40C°	-0.485	3.046	7.76	91.7	142.6
	50C°	-0.477	7.816	5.43	75.8	186.2
	60C°	-0.467	8.753	4.79	95.8	177.4
	70C°	-0.458	9.666	2.83	83.1	195.3

Table 6
Temperature influence on electrochemical parameters of carbon steel API5LX60 in 0.5 M H_2SO_4 in the presence of an inhibitor (4g/L).

Medium/ conc		E_{corr}(V)	I_{corr} (mA /cm^2)	R_P (Ω. cm^2)	β_a(mV/ dec)	-β_c(mV/ dec)	IE%
4g/ L	25C°	-0.468	0.104	107	52.4	135.3	85.41
	30C°	-0.472	0.140	201	51.0	139.0	92.25
	40C°	-0.477	0.099	194	68.7	135.5	96.74
	50C°	-0.486	0.435	108	66.5	129.8	94.43
	60C°	-0.496	0.855	68	62.7	126.7	90.23
	70C°	-0.515	1.202	35	68.2	141.5	87.56

Table 7
Electrochemical impedance parameters for the corrosion of carbon steel X 60 in 0.5 M H_2SO_4 at different temperatures.

H_2SO_4 (0,5M)	Rs (Ω. cm^2)	Rp (Ω. cm^2)	CPE_{dl} (mF.cm^{-2}) × 10^{-3}
25C°	3.779	27.22	0.580
30C°	2.809	17.55	0.781
40C°	2.443	14.89	0.876
50C°	2.857	9.28	0.939
60C°	3.809	7.89	0.980
70C°	4.585	6.92	1.364

Table 8
Electrochemical impedance parameters for the corrosion of API5L X 60 carbon steel in 0.5 M H_2SO_4+4g/L inhibitor at different temperatures.

4g/L	Rs (Ω. cm^2)	Rp (Ω. cm^2)	CPE_{dl} (mF.cm^{-2}) × 10^{-3}	IE%
25C°	2.353	170.8	0.432	84.06
30C°	2.429	228.9	0.407	92.33
40C°	2.261	409.6	0.356	96.36
50C°	2.341	168.2	0.668	94.48
60C°	2.854	83.9	0.707	90.60
70C°	3.100	64.9	0.735	89.34

Table 9
Activation parameters for adsorption of Olibanum on X60 carbon steel surface at different Temperatures.

Medium	E act (J.mol^{-1})	ΔH act (J.mol^{-1})	ΔS act (J.K^{-1}mol^{-1})
H_2SO_4 M	**19.640**	**63.701**	**-187.949**
4g/L	**18.884**	**58.398**	**-198.432**

$$\theta = \ln C_{inh} + K_{ads} \quad (7)$$

Where Cinh signifies the inhibitor concentration (g/L) and Kads denotes the adsorption/desorption equilibrium constant and ɵ is the surface coverage.

The linear plots have a slope of 0.567 and a regression coefficient (R^2) of 0.98. The plot's y intercept yields the Kads value where is equal: $K_{ads} = e^{\frac{Intercept}{Slope}}$ and their value is 17.27 L. g^{-1}.

The conventional Gibbs free energy of adsorption (ΔG° ads) is calculated using Kads, as illustrated below:

$$\Delta G^{\circ}ads = -RTln\,(K_{ads} \times C_{H2O}) \quad (8)$$

- R is the universal gas constant,
- T is the temperature in K (kelvin),
- C_{H2O} is equal 1000g.L^{-1}.

Gibbs free energy indicates a process of spontaneous and stable adsorption. The presence of physisorption, involves a minor electrostatic interaction between charged inhibitor molecules and the charged metal, is indicated if the ΔG°ads value drops below -20 kJ/mol.

When the ΔG°ads value drops below -40 kJ/mol, chemisorption has occurred, in which the inhibitor molecule forms a coordination bond with the metal surface. The coexistence of physisorption and chemisorption is confirmed when the ΔG°ads value is between -20 and -40 kJ/mol.

The obtained ΔG °ads value, derived from the Temkin isotherm, is -24,191kJ/mol, providing a both indication of physicochemical adsorption.

3.5. Surface morphology

The scanning electron microscopy (SEM) images of API5L X60 pipeline steel specimens submerged in 0.5 M H_2SO_4, both with and without Olibanum at a concentration of 4 g/L for a duration of 3 days, are depicted in Fig. 10

The SEM images reveal significant surface damage in the absence of an inhibitor (active corrosion) (Fig. 10.c, d). However, in the presence of the Olibanum inhibitor, the micrographs show a reduction in corrosion sites and pitting on the API5L X60 steel surface. This is attributed to the formation of a protective inhibitor layer on the metal surface (Fig. 10.e, f). These observations, supports the results obtained through the previous techniques.

3.6. Chemical analysis with (EDS)

EDS analysis was used to assess the components present on the surface of API 5LX60 steel after 72 hours in contact with 0.5M sulfuric acid with and without 4g/L Olibanum. Fig. 11 exhibits the microscope images and chemical analysis for the metal in the presence and absence of the inhibitor.

The results obtained in (Table 4) after introducing the metal into the sulfuric acid show a high quantity of iron (62.42%) and oxygen (26.91%) and carbon present only (8.34%). These results confirm iron dissolution (Fig. 11a). In the presence of Olibanum, it is clearly noticed that the increase in oxygene and carbon (43.64%,18.78%) respectively, while iron decrease up to (34.33%), which means that the inhibitor reduced the corrosion phenomenon, as can be seen in the microscope image (Fig. 11b).

3.7. Effect of temperature

3.7.1. Polarization curves

Fig. 12 show the polarization curve with and without inhibitors at different temperatures with a fixed concentration 4g/L.

Tables 5 and 6 shows the electrochemical parameters at different temperature such as Ecorr, Icorr, βa, βc, IE %.

As shown in Table 6, the value of i_{corr} increases from 0.713 mA cm^{-2} to 9.666 mA cm^{-2} in the absence of a corrosion inhibitor as the temperature rises. This demonstrates that higher temperatures, along with sulfuric acid and other corrosive agents significantly accelerate the corrosion of X60 steel. After addition of 4g/L of Olibanum, it clearly seen that at lower temperatures ranging from 25 to 40°C, the inhibition efficiency improved, due to occurrence of Olibanum adsorption on the surface of metal. These results show that temperature increases the inhibitory efficiency [39–41]. Hence, Increase in temperature increased the inhibition efficiencies of the Olibanum suggesting chemisorption of Olibanum components on the surface of the metals at the range 25-50°C [42–53].

In the acid solution containing 4g. L^{-1} of Olibanum, the corrosion

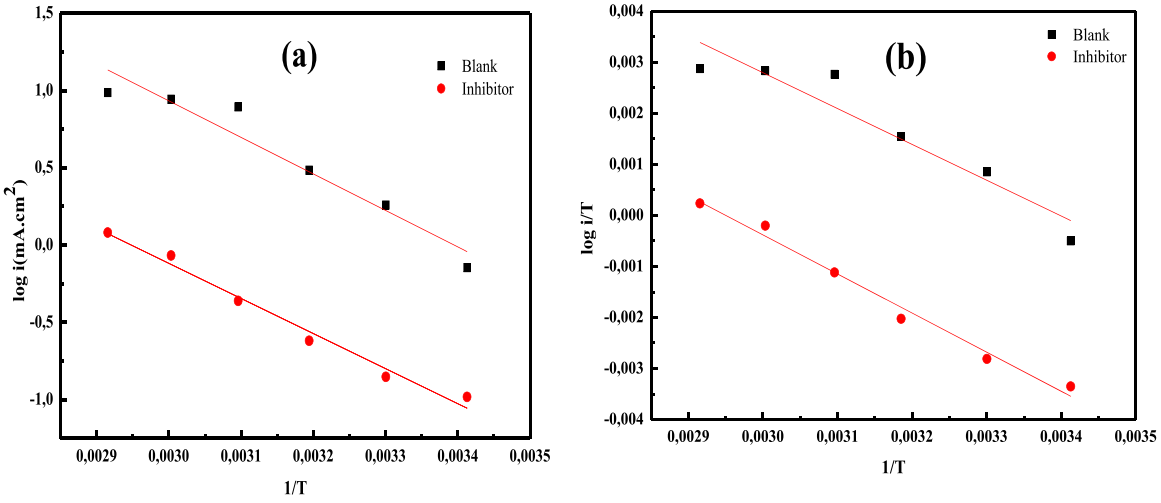

Fig. 14. a) Arrhenius plots of X60 carbon steel in 0.5 M H_2SO_4 and containing 4g/L of Olibanum at the temperature range of (298.15-343.15 K).b) Traces of the transition states in the absence and presence of 4g/L of Olibanum in 0.5M H_2SO_4 at different temperatures.

currents of X60 steel increase with temperature from 50°C to 70°C. This means that the number of adsorbed molecules decreases and the inhibition efficiency of the Olibanum decreases. Despite this behaviour, Olibanum exhibits satisfactory inhibition efficiencies even at higher temperatures (87% at 70°C) (Table 6). The increase in inhibition efficiency with increasing temperature can be explained by the solubility of the inhibitor, which increases at higher temperatures.

3.7.2. Electrochemical impedance (EIS)

Nyquist plots of API5LX60 steel in uninhibited and inhibited acidic solutions containing 0.5 M of sulfuric acid and Frankincence (4g/L) at temperatures of 25°C, 40°C,50°C, 60°C and 70°C are given in Fig. 13a and b, respectively.

Tables 7 and 8 lists the impedance parameters from the EIS method, including the double-layer capacitance CPE_{dl}, charge transfer resistance RP, and inhibition efficiency with and without inhibitor.

The analysis reveals that the Rp decreases while the CPE_{dl} rises as the temperature of the sulfuric acid medium rises; these findings indicate the presence of metallic dissolution. The decrease in charge transfer resistance is less in the inhibited medium, supporting the findings of the potentiodynamic polarization curve.

3.7.3. Temperature and activation experiments

The thermodynamic parameters for the corrosion reaction, such as activation energy (ΔEact), activation entropy (ΔSact), and activation enthalpy (ΔHact) (Table 9) ,were evaluated using the Arrhenius equation (Eq. 5) and the transition state equation (Eq. 6).

To obtain these parameters, corrosion current densities were measured from polarization curves across a temperature range of 298.15 to 343.15 K in a 0.5 M sulfuric acid solution, both without and with the Olibanum inhibitor. The Arrhenius plots, showing the relationship between log (icorr) and the inverse of temperature, were used to calculate the activation energies, revealing the influence of temperature and inhibitor concentration on the corrosion process (Fig. 14).

Absolute temperature in reciprocal terms:

$$logi_{corr} = logA - \frac{E}{2.303RT} \tag{9}$$

While the transition state equation can be defined as:

$$Icorr = \frac{RT}{Nh}\exp\left(\frac{\Delta S\ act}{R}\right)\exp\left(-\frac{\Delta H\ act}{RT}\right) \tag{10}$$

Where T is the absolute temperature, R = 8.32mol^{-1}. K^{-1} is the universal gas constant, h = 6.626×10^{-34}J.s is Plank's fundamental constant, and N = 6.02214076 × 1023 is Avogadro's number. The slope represents (-Ea /R) and the intercept (Ln R/Nh + ΔSa /R).

If the activation energy (Ea) of a corrosive solution increases after the addition of an inhibitor compared to an uninhibited solution, it signifies that the inhibitor is effective in mitigating metal corrosion. From a thermodynamic point of view, positive enthalpy changes (ΔH) reflect the endothermic nature of the steel dissolution process, with an increase in activation enthalpy (ΔH) corresponding to a decrease in metal dissolution, which is confirmed by the enthalpy value obtained. Furthermore, the high and negative entropy changes (ΔS) indicate a decrease in disorder during the conversion of the reactants into an activated iron molecular complex in solution.

In addition, the activation energy (Ea) without the inhibitor is 19.640 J/mol, while with the inhibitor it decreases slightly to 18.884 J/mol. This small decrease is explained by the inhibitor formation of a protective layer on the metal surface, suggesting a mechanism largely associated with physical adsorption, as chemical adsorption generally involves a more significant increase in Ea. The enthalpy of activation (ΔHact) is 63.701 J/mol for the corrosive solution and 58.398 J/mol for the inhibited solution. The activation entropy (ΔSact) is -187.949 J/K.mol for the corrosive medium and -198.423 J/K.mol for the inhibited solution. These negative values indicate a decrease in heterogeneity at the metal/solution interface, consistent with the formation of a more ordered adsorbed layer. In more detail, the free energy of adsorption (ΔG°ads) derived from the Temkin isotherm is -24.191 kJ/mol. This value falls within the range of -20 to -40 kJ/mol, which typically indicates mixed adsorption behaviour. In conclusion, the adsorption process in this system appears to be predominantly physical, characterised by the formation of a protective surface layer, with possible contributions from weak chemical binding interactions [54–56].

4. Conclusion

This study demonstrates the effectiveness of Olibanum as a green corrosion inhibitor for API5LX60 steel in 0.5M H_2SO_4. The key findings are as follows:

- Olibanum significantly reduces corrosion, with an inhibition efficiency of up to 84% at 4 g/L.
- Gravimetric analysis, Tafel polarization, and electrochemical impedance spectroscopy (EIS) confirm its strong protective properties.
- Adsorption on the steel surface follows the Temkin isotherm, indicating a mixed physicochemical interaction.
- SEM-EDS analysis reveals the formation of a protective layer, supporting its corrosion inhibition mechanism.
- Temperature enhances Olibanum's solubility, improving its inhibitory effect.
- As a non-toxic and sustainable inhibitor, Olibanum is a promising alternative for corrosion protection in acidic environments.

Declaration of ineterst statement

The present manuscript, or its contents in some other form, has not been published previously by any of the authors and/or is not under consideration for publication in another journal at the time of submission. All co-authors have agreed on its contents.

CRediT authorship contribution statement

Sobhi Nour El Houda: Writing – review & editing, Writing – original draft, Validation, Software, Resources, Methodology, Investigation, Data curation, Conceptualization. **Boukhouiete Amel:** Writing – review & editing, Validation, Supervision, Project administration.

Declaration of competing interest

The authors declare that they have no known competing financial interests or personal relationships that could have appeared to influence the work reported in this paper.

Acknowledgements

We are very thankful to the Algerian Ministry of Higher Education and Scientific Research (MESRS) and the general direction of research (DGRSDT) for their help and support.

References

[1] Al-Azawi KF, Mohammed IM, Al-Baghdadi SB, Salman TA, Issa HA, Al- Amiery AA, Gaaz TS, Kadhum AAH. Experimental and quantum chemical simulations on the corrosion inhibition of mild steel by 3-((5-(3, 5-dinitrophenyl)-1, 3, 4- thiadiazol-2-yl) imino) indolin-2-one. Results Phys 2018;9:278–83.
[2] Stenger F. Numerical methods based on sinc and analytic functions. Springer Science & Business Media; 2012 (Vol. 20).
[3] Alibakhshi E, Ramezanzadeh M, Bahlakeh G, Ramezanzadeh B, Mahdavian M, Motamedi M. Glycyrrhiza glabra leaves extract as a green corrosion inhibitor for mild steel in 1 M hydrochloric acid solution: Experimental, molecular dynamics, Monte Carlo and quantum mechanics study. J Mol Liq 2018;255:185–98.

[4] Zeino A, Abdulazeez I, Khaled M, Jawich MW, Obot IB. Mechanistic study of polyaspartic acid (PASP) as eco-friendly corrosion inhibitor on mild steel in 3% NaCl aerated solution. J Mol Liq 2018;250:50–62.
[5] Srivastava V, Haque J, Verma C, Singh P, Lgaz H, Salghi R, Quraishi MA. Amino acid based imidazolium zwitterions as novel and green corrosion inhibitors for mild steel: experimental, DFT and MD studies. J Mol Liq 2017;244:340–52.
[6] Tan B, Fu A, Guo L, Ran Y, Xiong J, Marzouki R, Li W. Insight into anti-corrosion mechanism of Dalbergia odorifera leaves extract as a biodegradable inhibitor for X70 steel in sulfuric acid medium. Ind Crops Prod 2023;194:116106.
[7] Tan B, Liu Y, Ren H, Gong Z, Li X, Li W, AlObaid AA. N, S-carbon quantum dots as inhibitor in pickling process of heat exchangers for enhanced performance in multi-stage flash seawater desalination. Desalination 2024;589:117969.
[8] El Houda SN, Amel B, Malika F. Trifolium repens extracts as a green corrosion inhibitor for carbon steel in a 3.5% NaCl solution. J Taiwan Inst Chem Eng 2024;165:105771.
[9] Chen J, Wu Y, Guo L, Li W, Tan B, Brahmia A. Insight into the anti-corrosion mechanism of Pisum Sativum L leaves extract as the degradable inhibitor for Q235 steel in sulfuric acid medium. J Taiwan Inst Chem Eng 2023;143:104664.
[10] Gu T, Tan B, Liu J, Chen J, Wei H, Zhang F, Li W. Insight into the corrosion inhibition performance of Jasmine flower extract on copper in sulfuric acid medium using experimental and theoretical calculation methods. J Taiwan Inst Chem Eng 2023;150:105047.
[11] Xu Z, Tan B, Zhang S, Chen J, Li W. Exploring of an ecological corrosion inhibitor of wood hibiscus leaf extract for the Cu/H2SO4 system based on experimental study and theoretical calculations. J Taiwan Inst Chem Eng 2023;143:104686.
[12] Hu P, Cheng P, Wu Y, Guo L, AlObaid AA. Insight into the corrosion inhibition performance of Capsicum annuum L. leaf extract as corrosion inhibitor for copper in sulfuric acid medium. J Taiwan Inst Chem Eng 2024;161:105558.
[13] Lai XB, Ngo KLD, Manh TD, Van Dinh T, Thu XNT, Nguyen DK, Dang NN. Inhibition properties of Vang tea-water extract for carbon steel corrosion in acidic environments. J Taiwan Inst Chem Eng 2023;149:104941.
[14] Wang Q, Wu X, Zheng H, Liu L, Zhang Q, Zhang A, Li X. Evaluation for Fatsia japonica leaves extract (FJLE) as green corrosion inhibitor for carbon steel in simulated concrete pore solutions. J Building Eng 2023;63. 105-568.
[15] Tran TN, Vu NSH, Tran TT, Jo DS, Huynh TL, Panaitescu C, Dang NN. Precise major compounds in Barringtonia acutangula flower–water extract for mitigating carbon steel corrosion. J Taiwan Inst Chem Eng 2024;155. 105-251.
[16] Xu Z, Tan B, Chen J, Liu J, Zheng X, Guo L, Li W. Insight into the anti-corrosion mechanism of Chinese mahonia leaves as a green and bio-degradable against copper corrosion in sulfuric acid medium. J Taiwan Inst Chem Eng 2023;150. 105-044.
[17] Döner A, Yıldız R, Arslanhan S, Baran MF. A comprehensive analysis of Arum dioscoridis plant leaf extract as a corrosion inhibitor for mild steel in 1 M HCl: Synthesis, characterization, surface analysis observations, experimental and DFT studies. J Taiwan Inst Chem Eng 2025;169:105–955.
[18] El-Hashemy MA, Almehmadi AM. Evaluation of Glebionis coronaria L. flower extract as a novel green inhibitor for mild steel corrosion in acidic environment. Biomass Convers Biorefin 2025;15(1):1121–37.
[19] Mamudu U, Santos JH, Umoren SA, Alnarabiji MS, Lim RC. Investigations of corrosion inhibition of ethanolic extract of Dillenia suffruticosa leaves as a green corrosion inhibitor of mild steel in hydrochloric acid medium. Corros Commun 2024;15:52–62.
[20] Nour-El-Houda SOBHI, Amel BOUKHOUIETE. Corrosion inhibition of API5L X60 steel in sulfuric acid using gum arabic. Rev Roum Chim 2023;68. 1-2.02.
[21] Barboza GK, de Oliveira MC, Neves MA, Echevarria A. Justicia brandegeeana as a green corrosion inhibitor for carbon steel in sulfuric acid. Green Chem Lett Rev 2024;17(1):2320254.
[22] Loto, R. T., Loto, C. A., Popoola, A. P. I., & Ranyaoa, M. Pyrimidine derivatives as environmentally-friendly corrosion inhibitors: A review, (2012).
[23] Millard S, Sadowski L. Novel method for linear polarisation resistance corrosion measurement. e-J Nondestructive Testing Ultrasonics 2009;14.
[24] Nyborg R. Controlling internal corrosion in oil and gas pipelines. Business Briefing: Exploration & Production: The Oil & Gas Review 2005;2:70–4.
[25] Oni BO, Egiebor NO, Ekekwe NJ, Chuku A. Corrosion behavior of tin-plated carbon steel and aluminum in NaCl solutions using electrochemical impedance spectroscopy. J Minerals Mater Characterization Eng 2008;7(04):331.
[26] Sastri VS. Green corrosion inhibitors: theory and practice. John Wiley & Sons; 2012.
[27] Pasquini C. Near infrared spectroscopy : fundamentals, practical aspects and analytical applications. J Braz Chem Soc 2003;14:198–219.
[28] Al-Dahmash ND, Al-Ansari MM, Al-Otibi FO, Singh AR. Frankincense, an aromatic medicinal exudate of Boswellia carterii used to mediate silver nanoparticle synthesis: Evaluation of bacterial molecular inhibition and its pathway. J Drug Deliv Sci Technol 2021;61:102–337.
[29] SOBHI NH, BOUKHOUIETE A. Corrosion inhibition of api5l x60 steel in sulfuric acid using gum arabic. Rev Roum Chim 2023;68(1-2):17–25.
[30] Gupta M, Kumar S, Kumar R, Kumar A, Verma R, Darokar MP, Pal A. Inhibition of heme detoxification pathway in malaria parasite by 3-hydroxy-11-keto-β-boswellic acid isolated from Boswellia serrata. Biomed Pharmacother 2021;144:112–302.
[31] Golestani G, Shahidi M, Ghazanfari D. Electrochemical evaluation of antibacterial drugs as environment-friendly inhibitors for corrosion of carbon steel in HCl solution. Appl Surf Sci 2014;308:347–62.
[32] Rotaru I, Varvara S, Gaina L, Muresan LM. Antibacterial drugs as corrosion inhibitors for bronze surfaces in acidic solutions. Appl Surf Sci 2014;321:188–96.
[33] Tan B, Ren H, Yin C, Li X, Li X, Wang R, Al-Sadoon MK. Nepeta cataria L. leaf extracts as eco-conscious corrosion inhibitor for copper in H2SO4 medium. Colloids and Surfaces A: Physicochem Eng Aspects 2025:136399.
[34] Tan B, Ren H, Zhang R, Wang R, Ma L, Li X, Al-Sadoon MK. A novel corrosion inhibitor for copper in sulfuric acid media: complexation of iodide ions with Benincasa Hispida leaf extract. Colloids and Surfaces A: Physicochem Eng Aspects 2025;705:135710.
[35] Ji G, Anjum S, Sundaram S, Prakash R. Musa paradisica peel extract as green corrosion inhibitor for mild steel in HCl solution. Corros Sci 2015;90:107–17.
[36] Hegazy MA, Abdallah M, Awad MK, Rezk M. Three novel di-quaternary ammonium salts as corrosion inhibitors for API X65 steel pipeline in acidic solution. Part I: experimental results. Corros Sci 2014;81:54–64.
[37] Thanapackiam P, Rameshkumar S, Subramanian SS, Mallaiya K. Electrochemical evaluation of inhibition efficiency of ciprofloxacin on the corrosion of copper in acid media. Mater Chem Phys 2016;174:129–37.
[38] Mobin M, Zehra S, Parveen M. L-Cysteine as corrosion inhibitor for mild steel in 1 M HCl and synergistic effect of anionic, cationic and non-ionic surfactants. J Mol Liq 2016;216:598–607.
[39] Mourya P, Banerjee S, Rastogi RB, Singh MM. Inhibition of mild steel corrosion in hydrochloric and sulfuric acid media using a thiosemicarbazone derivative. Ind Eng Chem Res 2013;52(36):12733–47.
[40] Srivastava V, Haque J, Verma C, Singh P, Lgaz H, Salghi R, Quraishi MA. Amino acid based imidazolium zwitterions as novel and green corrosion inhibitors for mild steel: Experimental, DFT and MD studies. J Mol Liq 2017;244:340–52. 2017.
[41] Wang J, Ma X, Tabish M, Wang J. Sunflower-head extract as a sustainable and eco-friendly corrosion inhibitor for carbon steel in hydrochloric acid and sulfuric acid solutions. J Mol Liq 2022;367:120–429.
[42] Pham TH, Lee WH, Kim JG. Chrysanthemum coronarium leaves extract as an eco-friendly corrosion inhibitor for aluminum anode in aluminum-air battery. J Mol Liq 2022;347:118–269.
[43] Aksamija A. Étude chimique des matériaux résineux: oliban, dammar et mastic: application à des prélèvements artistiques et archéologiques. (Doctoral dissertation, Université d'Avignon); 2012.
[44] Marušić K, Otmačić Ćurković H. Self-assembling monolayers of stearic acid in protection of steel. Croat Chem Acta 2018;91(4):427–33.
[45] Ansari KR, Ramkumar S, Nalini D, Quraishi MA. Studies on adsorption and corrosion inhibitive properties of quinoline derivatives on N80 steel in 15% hydrochloric acid. Cogent Chem 2016;2(1):1145032.
[46] Hoai Vu NS, Hien PV, Mathesh M, Hanh Thu VT, Nam ND. Improved corrosion resistance of steel in ethanol fuel blend by titania nanoparticles and Aganonerion polymorphum leaf extract. ACS Omega 2019;4(1):146–58.
[47] Zhang W, Liu Y, Zhang Y, Wang LJ, Wu YC, Li HJ. 9-Substituted acridines as effective corrosion inhibitors for mild steel: electrochemical, surface morphology, and computational studies. New J Chem 2020;44(16):6464–74.
[48] Torres VV, Amado RS, De Sá CF, Fernandez TL, da Silva Riehl CA, Torres AG, D'Elia E. Inhibitory action of aqueous coffee ground extracts on the corrosion of carbon steel in HCl solution. Corros Sci 2011;53(7):2385–92.
[49] Pereira SSDAA, Pegas MM, Fernandez TL, Magalhaes M, Schöntag TG, Lago DC, D'Elia E. Inhibitory action of aqueous garlic peel extract on the corrosion of carbon steel in HCl solution. Corros Sci 2012;65:360–6.
[50] Yahiya S, Othman NK, Daud AR, Jalar A, Ismail R. The influence of temperature on the inhibition of carbon steel corrosion in acidic lignin. Anti-Corrosion Methods and Materials 2015.
[51] Umoren SA, Obot IB, Ebenso EE, Okafor PC, Ogbobe O, Oguzie EE. Gum arabic as a potential corrosion inhibitor for aluminium in alkaline medium and its adsorption characteristics. Anti-Corrosion Methods and Materials 2006;53(5):277–82.
[52] El-Etre AY. Inhibition of aluminum corrosion using Opuntia extract. Corros Sci 2003;45(11):2485–95.
[53] Abdallah M. Corrosion inhibition of steel by 1-phenyl 5-mercapto 1, 2, 3, 4-tetrazole in acidic environments. Corros Sci 2004;46. 1981.
[54] Saha P, Chowdhury S. Insight into adsorption thermodynamics. Thermodynamics 2011;16:349–64.
[55] Ebelegi AN, Ayawei N, Wankasi D. Interpretation of adsorption thermodynamics and kinetics. Open J Phys Chem 2020;10(3):166–82.
[56] Das B, Mondal NK, Bhaumik R, Roy P. Insight into adsorption equilibrium, kinetics and thermodynamics of lead onto alluvial soil. Int J Environ Sci Technol 2014;11:1101–14.